

Short communication

## Stability and robustness of metal-supported SOFCs

Michael C. Tucker\*, Grace Y. Lau, Craig P. Jacobson,  
Lutgard C. DeJonghe, Steven J. Visco

*Materials Sciences Division, Lawrence Berkeley National Laboratory, 1 Cyclotron Road,  
Berkeley, CA 94720, United States*

Received 30 August 2007; received in revised form 14 September 2007; accepted 14 September 2007  
Available online 18 September 2007

### Abstract

Tubular metal-supported SOFCs with YSZ electrolyte and electrodes comprising porous YSZ backbone and infiltrated Ni and LSM catalysts are operated at 700 °C. Tolerance to five complete anode redox cycles and five very rapid thermal cycles is demonstrated. The power output of a cell with as-infiltrated Ni anode degrades rapidly over 15 h operation. This degradation can be attributed primarily to coarsening of the fine infiltrated Ni particles. A cell in which the infiltrated Ni anode is pre-coarsened at 800 °C before operation at 700 °C shows dramatically improved stability. Stable operation over 350 h is demonstrated.

Published by Elsevier B.V.

*Keywords:* SOFC; Metal support; Stability

### 1. Introduction

Metal-supported SOFCs are very attractive due to their low materials cost, inherent robustness, and expected manufacturability. The cell design described here comprises YSZ electrolyte cosintered with metal support, and electrocatalysts infiltrated after the high-temperature sintering steps. Co-sintering the electrolyte enables the use of high-throughput, inexpensive deposition techniques such as screen-printing, aerosol spray, and dipcoating, which provide a thin electrolyte layer (i.e. 5–20 μm thick). Such a thin electrolyte allows high performance to be achieved in the 650–700 °C temperature range, suitable for long-term operation of the metal support.

Rapid improvement in power density has resulted in over 1 W cm<sup>-2</sup> power generation at 700 °C for this design, as described previously [1]. Such high power density was achieved at relatively low temperature because of the thin electrolyte and the very large triple-phase boundary presented by infiltrated LSM and Ni catalysts. In this work, redox cycling capability and rapid thermal cycling tolerance of this cell design are demonstrated. Of course, stability is also critical to commercial

viability. This work describes one method of improving the stability of a metal-supported cell with infiltrated anode and cathode.

### 2. Experimental methods

Tubular metal-supported fuel cells comprising porous metal/porous YSZ/dense YSZ/porous YSZ/porous metal were fabricated, brazed to cell housing and gas manifold, and infiltrated with catalysts as described elsewhere [1]. The cells produced here had LSM on the inside of the tube and Ni on the outside, although this orientation can easily be switched during the infiltration step. Catalysts were introduced by infiltrating LSM twice and Ni 10 times.

Small specimens of porous YSZ were infiltrated 10 times with Ni. The effect of pre-coarsening on Ni particle size was assessed by firing these specimens at various temperatures for 4 h in 4% H<sub>2</sub>/96% Ar, and observing the resulting microstructure with SEM. Cells were then prepared with pre-coarsened Ni anodes. Ni was infiltrated 10 times, with conversion of Ni-nitrate to Ni-oxide accomplished after each infiltration step by firing the cell in air at 650 °C. The nitrate-oxide conversion can be accomplished at as low a temperature as 300 °C. This was followed by pre-coarsening the cell by firing at various temperatures for 4 h in 4% H<sub>2</sub>/96% Ar. This infiltration-precoarsening cycle

\* Corresponding author. Tel.: +1 510 486 5304; fax: +1 510 486 4881.  
E-mail address: [mctucker@lbl.gov](mailto:mctucker@lbl.gov) (M.C. Tucker).

was repeated three times for each cell. LSM was infiltrated into the cathode side of the cell after the pre-coarsening steps so as to avoid decomposition of the LSM in the reducing atmosphere.

Planar anode-supported cells were prepared as follows. NiO (J.T. Baker) and YSZ [8Y, Tosoh Corp.] in a weight ratio of 1:1 were attritor-milled in isopropanol, using zirconia balls as the milling medium. Dried powder mixtures were uniaxially pressed and bisque fired at 1100 °C for 1 h. YSZ electrolytes were formed on the NiO–YSZ anode supports by aerosol colloidal deposition [2], and were co-sintered in air at 1400 °C for 4 h. A suspension of YSZ and polymer poreformer was then colloidal deposited onto the YSZ electrolyte with an area of 1 cm<sup>2</sup>. The resulting trilayer structure was sintered in air at 1275 °C for 4 h. Platinum-paste current collectors were placed on the electrodes, and then fired on at 900 °C for 0.5 h. LSM precursor solution was infiltrated into the porous YSZ layer and converted to LSM by heating at 650 °C for 0.5 h, as described elsewhere [3,4].

Redox cycling for the anode-supported and metal-supported cells proceeded by changing the anode gas stream from moist hydrogen to an argon purge, and then to air. Airflow was maintained for 10–15 min, much longer than necessary for complete oxidation of the Ni in the anode structure. During oxidation, ac impedance of the cell was monitored. It increased rapidly during the first couple minutes of oxidation and then became stable, indicating complete oxidation. The anode chamber was then again purged with argon and moist hydrogen flow was resumed. Open circuit potential and galvanostatic polarization behavior were assessed after each redox cycle.

Thermal cycling of the metal-supported cell was achieved by rapidly pulling the cell and test rig out of the furnace, letting it cool for several minutes to <100 °C and then rapidly replacing the cell and rig into the furnace. The cooling and heating rate were limited by the thermal mass of the test rig. Nonetheless, initial heating and cooling rates of >350 °C min<sup>-1</sup> were achieved.

Polarization curves were obtained using LabView software controlling a power supply (Kepco). ac impedance spectra were obtained with a potentiostat/frequency response analyzer (Solartron 1286/1255) in frequency sweep mode from 10<sup>6</sup> to 0.1 Hz. Fuel was hydrogen passed through a water bubbler at room temperature.

SEM/EDS analysis was obtained with a Hitachi S-4300SE/N scanning electron microscope in secondary electron imaging mode.

### 3. Results and discussion

Metal-supported SOFCs are expected to be more abuse-tolerant than other types of SOFCs because the metal support imparts structural robustness to the cell. The metal-supported cell structure developed at LBNL has been described previously [1]. The cell consists of porous ferritic stainless steel support and current collector, thin YSZ electrolyte, and porous YSZ electrode layers. The electrode layers are infiltrated with LSM and Ni catalysts after the high-temperature reducing-atmosphere firing steps required to prepare the cell structure. This avoids decom-

position of LSM, interdiffusion of Ni and FeCr, and extreme coarsening of Ni, all of which would be expected if the cell structure were sintered with the catalysts in place. Another benefit of this approach is that the mechanical integrity of the cell relies only on stainless steel and YSZ; Ni and LSM catalysts are not structural elements. Therefore, redox cycling of Ni will not compromise the cell structure, and thermal stress upon heating and cooling can be minimized by choosing a metal support with good CTE match with YSZ, such as ferritic stainless steel. Redox and thermal shock tolerance of metal-supported cells with infiltrated electrocatalysts are demonstrated below.

Fig. 1 compares the behavior of metal-supported and anode-supported cells upon complete redox cycling. Oxidation and reduction of the Ni catalyst was accomplished by switching the fuel stream between air and moist hydrogen, allowing enough time for complete NiO/Ni conversion at each step. The electrolyte film of the anode-supported cell cracked after only one redox cycle, leading to a low OCV (0.75 V) and concomitant greatly reduced power density. After two redox cycles, the electrolyte film was so cracked that only minimal power could be obtained from the cell. The anode-supported electrolyte film cracked due to being held in tension by the large volume expansion associated with the oxidation of Ni. Fig. 2 shows some of the cracks observed in the electrolyte after two complete redox cycles. This phenomenon has been discussed extensively elsewhere [5,6]. In contrast, the metal-supported cell does not fail after redox cycling. Oxidation of the infiltrated Ni catalyst does not affect the metal/YSZ structure of the cell and therefore does not exert a stress on the electrolyte film. The power density decreases slowly with each complete redox cycle, presumably arising from damage to the continuous network of Ni that coats the porous YSZ in the anode layer. From an operation standpoint, robustness to Ni oxidation would eliminate the need for anode blanketing gas on startup and cool-down and allow very

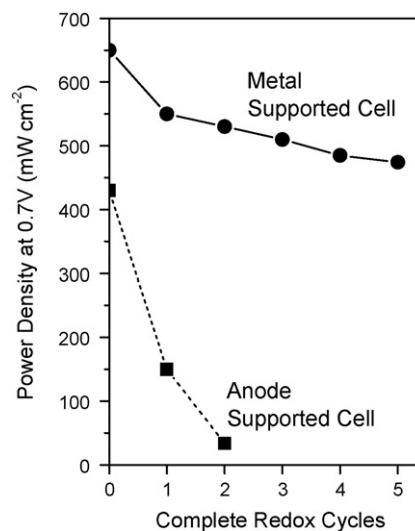


Fig. 1. Comparison of redox cycling stability for anode-supported (squares) and metal-supported (circles) cells. Cell was held at 700 °C while anode gas stream was switched between moist hydrogen and air. Oxidant was air and oxygen for anode-supported and metal-supported cells, respectively.

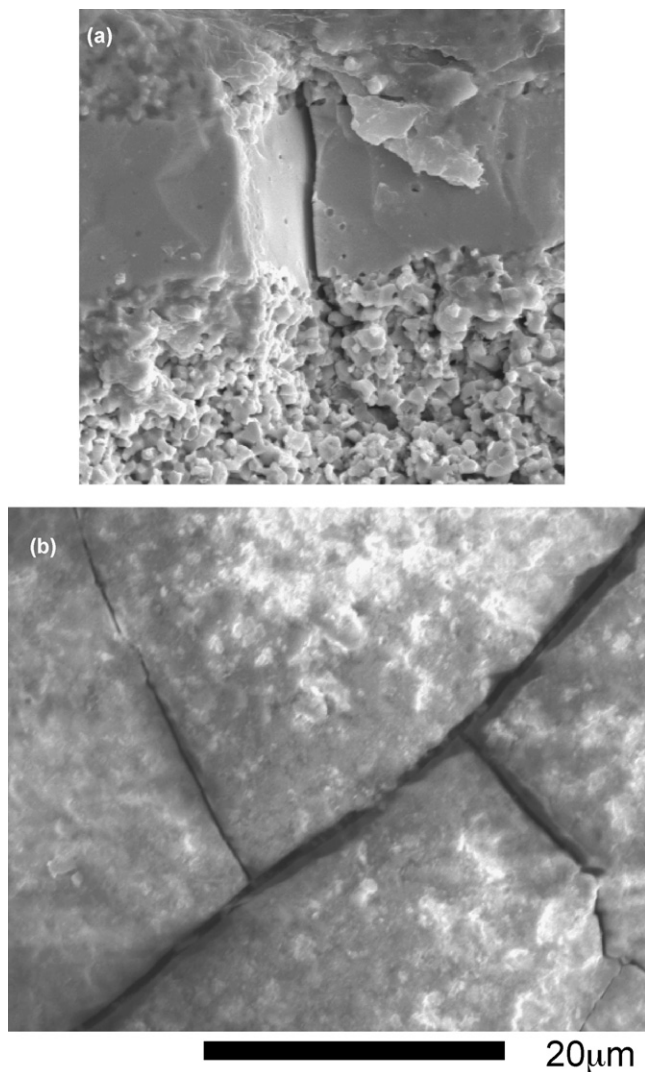


Fig. 2. SEM images of (a) cross-section view and (b) top-down view of cracks in anode-supported electrolyte film after redox cycling.

high fuel utilization without concern for structural integrity of the cell.

Rapid thermal cycling of a metal-supported cell structure has been demonstrated previously [7]. In that work, a braze-sealed cell was subjected to over 30 extremely rapid thermal cycles without loss of sealing. Here, the effect of thermal cycling on electrochemical performance is investigated. A metal-supported cell with brazed seals and infiltrated Ni and LSM catalysts was subjected to five rapid thermal cycles. Fig. 3a shows the temperature profile of the cell for a single cycle. Maximum heating and cooling rates of  $>350\text{ }^{\circ}\text{C min}^{-1}$  were achieved. Fig. 3b shows a slight decline in cell performance after each cycle. We suspect a large portion of this performance drop is in fact unrelated to thermal cycling, but rather due to coarsening of the fine Ni catalyst, as discussed below. In contrast, an anode-supported cell subjected to similar thermal cycling exhibited structural failure after only one cycle [7].

Clearly, metal-supported SOFCs are very abuse-tolerant. This allows for rapid startup, simplified balance of plant, and tolerance to unintended fluctuations in operational parameters

such as temperature, fuel flow rate, fuel utilization, etc. Further improvement of the redox and thermal cycling tolerance above that demonstrated here is desirable and will be the subject of future work.

Previous work has demonstrated stable performance for both cathodes comprising LSM infiltrated into porous YSZ, and for metal-supported cells with plasma-sprayed Ni–YSZ anode [3,8]. Therefore, it is not surprising that the unproven infiltrated Ni anode limits the stability of the present cell design, as discussed below. Fig. 4 shows the rapid power degradation of a metal-supported cell with infiltrated LSM and Ni catalysts. The catalysts were converted from nitrate salt precursors to oxides at  $650\text{ }^{\circ}\text{C}$  before cell operation. Therefore, the operating temperature of  $700\text{ }^{\circ}\text{C}$  was the highest temperature experienced by the catalysts. This allows for a very fine catalyst structure, providing high performance. Upon cell operation, the infiltrated NiO is reduced to Ni with particle size in the range 40–100 nm [1]. In the fuel environment, coarsening of these very fine Ni particles is a concern. Fig. 5 shows that changes in the Ni catalyst are indeed responsible for the rapid power degradation shown in Fig. 4. After cell heat-up and before passing current, the initial full cell impedance was found to be about  $0.9\text{ }\Omega\text{ cm}^2$ . After the 15 h of cell operation shown in Fig. 4, both the ohmic and electrode impedances increased dramatically. Suspecting

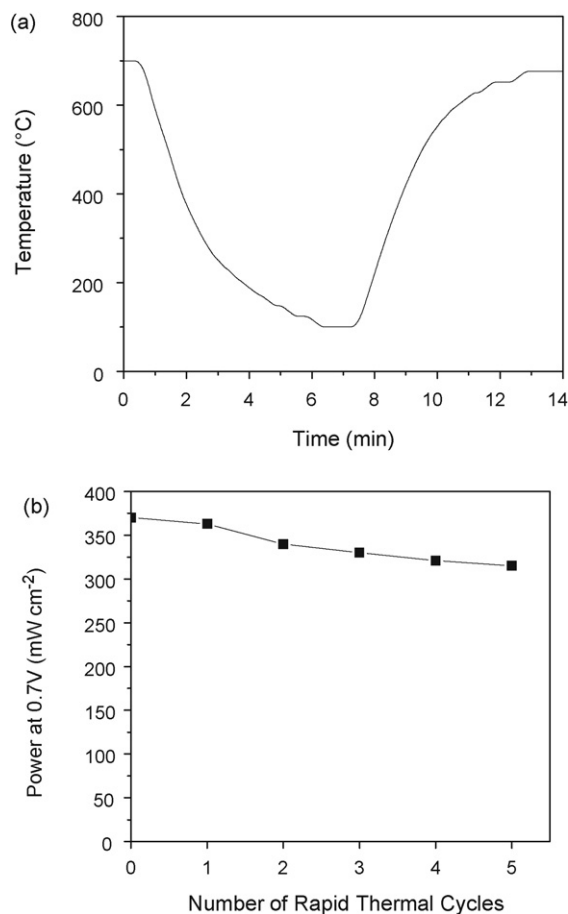


Fig. 3. Rapid thermal cycling of tubular metal-supported cell. (a) Temperature profile of cell during one complete thermal cycle. (b) Power retention upon multiple thermal cycles. Fuel is moist hydrogen, oxidant is oxygen.



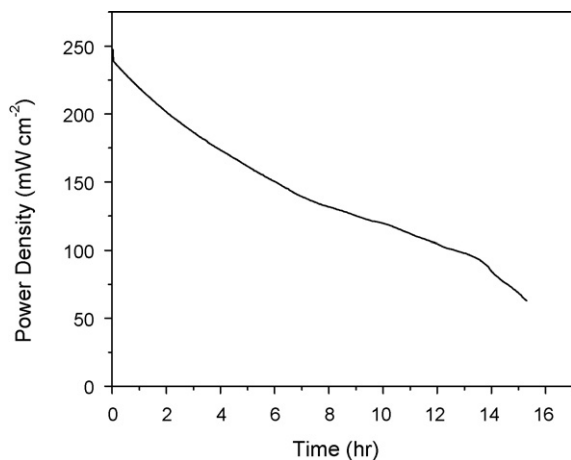


Fig. 4. Operation of tubular metal-supported SOFC with as-infiltrated Ni anode at  $300 \text{ mA cm}^{-2}$ ,  $700^\circ\text{C}$  with moist hydrogen as fuel and oxygen as oxidant.

the anode to be responsible for the observed degradation, the cell was then cooled and the anode was re-infiltrated with additional fine Ni catalyst to repair any damage to the Ni network caused by coarsening or dewetting from the YSZ backbone. After heating the cell to operating temperature, complete recovery and in fact slight improvement of the impedance was observed. Simply adding more Ni to the anode mitigated all the degradation observed during operation. This clearly indicates that changes in the Ni catalyst network caused degradation, and that the operation did not degrade other cell components, including the cathode, electrolyte, and seal.

We surmise that coarsening is a dominant cause of degradation of the initially very fine Ni catalyst. Presumably, pre-coarsening the Ni structure at a temperature above the operation temperature before operation would provide a more stable structure. Fig. 6 shows the extent of Ni coarsening at different temperatures. Porous YSZ structures were infiltrated with Ni, and then reduced for 4 h at various temperatures in  $4\% \text{ H}_2/\text{Ar}$ . Even after treatment at  $700^\circ\text{C}$  the Ni particles are much larger than the  $40\text{--}100 \text{ nm}$  particles found without any pre-coarsening step [1]. Particles larger than  $1 \mu\text{m}$  are observed after treatment at  $900^\circ\text{C}$ , and significant rounding of the particles occurs after  $1000^\circ\text{C}$  treatment. One consequence of the Ni coarsening/agglomeration is elimination of three-phase boundary. The largest coarsened particles are well within the range of Ni particle size found in typical Ni–YSZ cermet anodes, however, so this is of little concern. More problematic is the loss of connectivity in the Ni network. After pre-coarsening at  $1000^\circ\text{C}$ ,

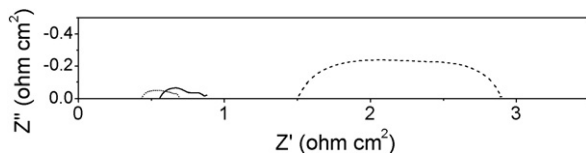


Fig. 5. Full-cell ac impedance spectra of a metal-supported SOFC with infiltrated LSM cathode and infiltrated Ni anode operating at  $700^\circ\text{C}$  with oxygen as oxidant and moist hydrogen as fuel. Solid line: as-infiltrated; dashed line: after 15 h operation as shown in Fig. 4; dotted line: after cooling cell, refreshing anode with additional Ni infiltration, and heating back up.

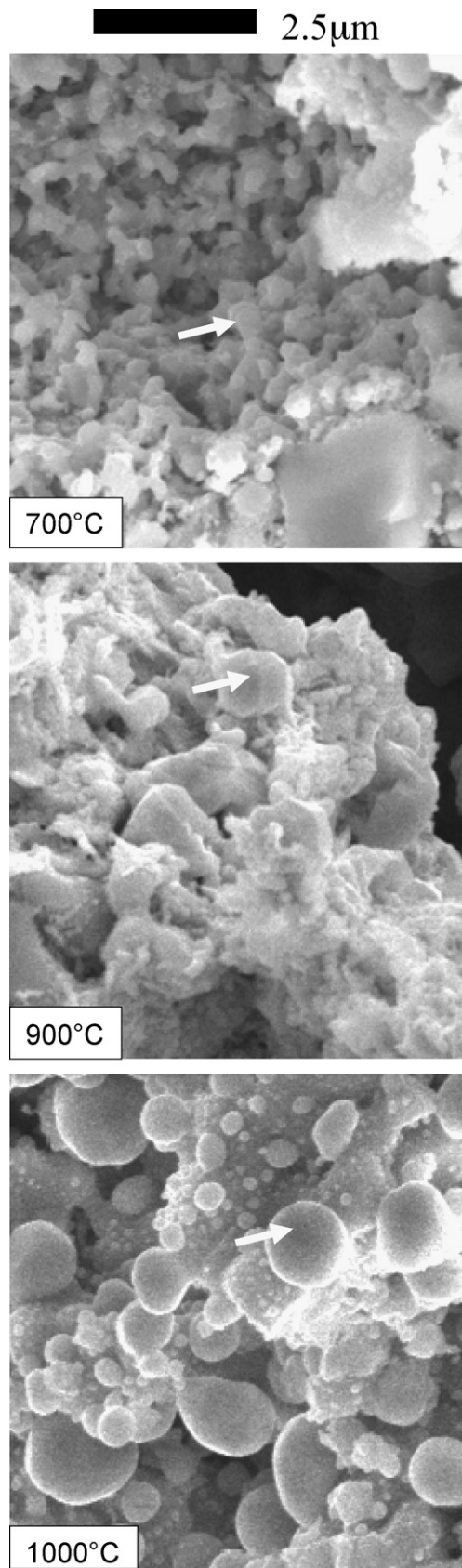


Fig. 6. SEM images of porous YSZ with infiltrated Ni after pre-coarsening for 4 h in  $4\% \text{ H}_2/96\% \text{ Ar}$  at  $700$ ,  $900$ , and  $1000^\circ\text{C}$ . The arrows indicate Ni particles.

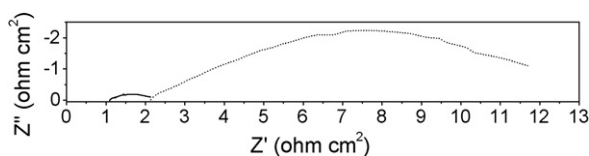


Fig. 7. Full-cell ac impedance spectra of a metal-supported SOFC with infiltrated LSM cathode and infiltrated Ni anode operating at 700 °C with oxygen as oxidant and moist hydrogen as fuel. Solid line: infiltrated Ni pre-coarsened at 800 °C; dotted line: infiltrated Ni pre-coarsened at 1000 °C.

the Ni particles are completely disconnected from each other; this is clearly detrimental for efficient removal of electrons from the anode layer. Therefore, multiple infiltration/reduction cycles were utilized to build up a more continuous network of pre-coarsened Ni particles. Fig. 7 shows the impedance of two cells with anodes produced in this way. After firing the YSZ and stainless steel components of the cell, Ni was infiltrated into the anode. The cells were then reduced at 800 or 1000 °C to pre-coarsen the Ni. This infiltration/reduction was carried out three times in total, after which LSM was infiltrated into the cathodes and cell testing proceeded. Although multiple infiltration steps were required to infiltrate the catalysts, these steps can be accomplished at high-throughput. Nitrate conversion occurs at low temperature (>300 °C required) and the ability of the metal-supported cell to withstand very rapid thermal cycling enables this thermal treatment to be very fast.

The impedance spectra shown in Fig. 7 clearly indicate the effect of pre-coarsening temperature on Ni performance. Pre-coarsening results in much larger ohmic and electrode impedances compared to the cell with as-infiltrated anode (Fig. 5). We expect this is due to the larger size and reduced connectivity of the Ni particles. Presumably the ohmic impedance could have been minimized by infiltrating more Ni, at the expense of manufacturability due to the excessive number of infiltration steps required. The impedance of the cell pre-coarsened at 1000 °C was too high to warrant further investigation.

Pre-coarsening at 800 °C allowed moderate performance to be achieved. The initial maximum power density was 145 mW cm<sup>-2</sup> at an operating temperature of 700 °C. The cell was operated at a constant current of 100 mA cm<sup>-2</sup> for 350 h, as shown in Fig. 8. Operating current densities for both the as-infiltrated and pre-coarsened cells were chosen to set the initial cell potential around 0.8 V, a realistic potential for high fuel

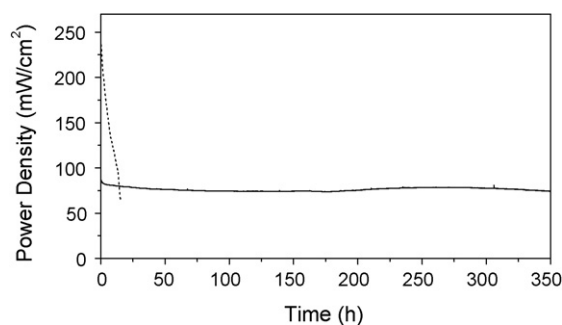


Fig. 8. Operation of tubular metal-supported SOFCs at 700 °C with moist hydrogen as fuel and oxygen as oxidant. Dashed line: as-infiltrated Ni anode, 300 mA cm<sup>-2</sup>; solid line: Ni anode pre-coarsened at 800 °C, 100 mA cm<sup>-2</sup>.

efficiency operation. This resulted in the different operating current densities for the two cells presented in Fig. 8. Oxygen was chosen as oxidant in order to alleviate the mass transport restriction observed previously when operating with air as oxidant [1]. Greatly improved stability was observed, as compared to the cell with no pre-coarsening step. This limited the Pre-coarsening the infiltrated Ni catalyst at a temperature above the operating temperature effectively stabilized the Ni microstructure. The observed cell stability also gives confidence in the potential longevity of the infiltrated cathode, cell structure, and braze seal. Of course, this stability has been achieved at the expense of performance. Continuing work is focused on achieving stable high performance.

#### 4. Conclusions

Promising stability of a metal-supported SOFC with co-intered YSZ electrolyte and infiltrated anode and cathode has been demonstrated at 700 °C. The stability of a cell with as-infiltrated Ni particles providing electronic connectivity and catalysis in the anode is poor. We presume this is due to coarsening of the Ni catalyst during operation, which leads to disconnection of the Ni network current path. Pre-coarsening the infiltrated Ni in reducing atmosphere at a temperature above the cell operation temperature promotes rapid particle growth, leading to greatly improved stability during operation. This pre-coarsening also disconnects the Ni network, so three infiltration-pre-coarsening cycles were used to build up a connected network of coarse, stable Ni particles. The performance of such a pre-coarsened infiltrated anode is lower than that of an as-infiltrated anode with no pre-coarsening. Future work will focus on demonstrating a stable, high-performance infiltrated anode.

#### Acknowledgements

The authors gratefully acknowledge the assistance of James Wu with vacuum brazing and Teresa Chen with catalyst infiltration.

This work was supported in part by the U.S. Department of Energy under Contract No. DE-AC02-05CH11231.

#### References

- [1] M.C. Tucker, G.Y. Lau, C.P. Jacobson, L.C. DeJonghe, S.J. Visco, J. Power Sources 171 (2007) 477–482.
- [2] S. De Souza, S.J. Visco, L.C. De Jonghe, J. Electrochem. Soc. 144 (3) (1997) 35–37.
- [3] T.Z. Sholklapper, V. Radmilovic, C.P. Jacobson, S.J. Visco, L.C. DeJonghe, Electrochem. Solid State Lett. 10 (4) (2007) B74–B76.
- [4] T.Z. Sholklapper, C. Lu, C.P. Jacobson, S.J. Visco, L.C. DeJonghe, Electrochem. Solid State Lett. 9 (8) (2006) A376–A378.
- [5] M. Cassidy, G. Lindsay, K. Kendall, J. Power Sources 61 (1996) 189–192.
- [6] J. Malzbender, E. Wessel, R. Steinbrech, Solid State Ionics 176 (29/30) (2005) 2201–2203.
- [7] M.C. Tucker, C.P. Jacobson, L.C. DeJonghe, S.J. Visco, J. Power Sources 160 (2) (2006) 1049–1057.
- [8] T. Franco, K. Schibinger, Z. Ilhan, G. Schiller, A. Venskutonis, ECS Trans. 7 (1) (2007) 771–780.